Photoinduced Oxetane Formation between 2-Norbornanone and Derivatives with Electron-Poor Ethylenes

Nicholas J. Turro* and George L. Farrington

Contribution from the Chemistry Department, Columbia University, New York, New York 10027. *Received February 15, 1980*

Abstract: The influence of steric hindrance on oxetane formation has been investigated in the photocycloadditions of *trans*-dicyanoethylene (*t*-DCE) to norcamphor (**K1**), spiro[cyclopropane-1,7′-norbornan]-2′-one (**K2**), and 7,7-dimethylnorcamphor (**K3**). The quantum yield for oxetane formation was found to increase with increasing steric hindrance toward exo approach of the olefin, i.e., ϕ_{ox}(**K3**) > ϕ_{ox}(**K2**) > ϕ_{ox}(**K1**). Evidence from GLC analysis and a NMR spectral investigation of the reaction mixtures was consistent with the stereospecific formation of four *trans*-dicyanooxetane products from the photocycloaddition of *t*-DCE to each ketone. The two major products in each case were identified as arising from exo attack of the olefin (endo oxetane oxygen configuration). In contrast to the product distributions observed with sodium borohydride reductions, blocking of the exo carbonyl face does not significantly increase the proportion of products resulting from an endo attack by *t*-DCE on the 2-norbornanone n,π^* singlets.

Oxetane Formation from 2-Norbornanones and *trans*-Dicyanoethylene. Steric Effects

A comparison of the rate constants for quenching of the fluorescence of substituted 2-norbornanones by *trans*-dicyanoethylene (*t*-DCE) and for their reduction by sodium borohydride ($NaBH_4$) suggests that the two processes are governed by similar steric requirements.[1,2] Bulky groups which increase the steric hindrance above the exo face of the carbonyl interfere with the approach of *t*-DCE to the π system of the n, π^* excited state and likewise with the delivery of hydride to the carbonyl ground state, resulting in a decrease in both the rates of fluorescence quenching (k_q^f) and reduction ($k_{red}^{NaBH_4}$).[2]

In addition to decreasing the overall rate of $NaBH_4$ reduction, substituent steric effects influence the product distribution by changing the relative rates for exo and endo attack on the carbonyl. This was observed in the series of norcamphor (**K1**), 7,7-dimethylenenorcamphor (**K2**), and 7,7-dimethylnorcamphor (**K3**), which respectively present minimal, intermediate, and relatively high degrees of steric hindrance toward exo approach.[2] The $NaBH_4$ reduction of norcamphor occurs preferentially from the exo approach to give the endo alcohol as the major product.[1] The endo alcohol is also the major product from **K2** as expected from its reduction rate, which is similar to that of **K1**. Blocking of the exo carbonyl face in **K3** is sufficiently severe to favor endo attack, and the exo alcohol is consequently the major product.

The similarity in the response of k_q^f and $k_{red}^{NaBH_4}$ to substituent steric hindrance allows prediction of the favored product stereochemistry from the photocycloaddition of *t*-DCE to **K1**–**K3** (eq 1–3).

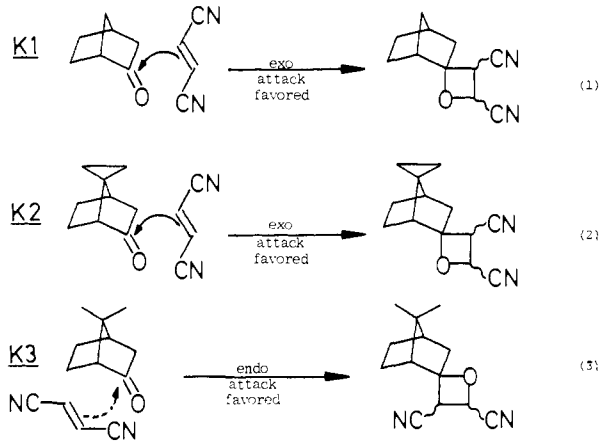

In each case the oxetane oxygen would be expected to have the same endo/exo stereochemistry as the major product alcohol from the $NaBH_4$ reduction.

Interpretation of the sodium borohydride reduction data is relatively uncomplicated; the reaction is irreversible and involves a single transition state, and, because the reaction is kinetically controlled, the ratio of product alcohols is a direct reflection of the rates of endo and exo attack. In contrast, since an exciplex intermediate is proposed to occur in the cycloadditions of alkanones to *t*-DCE,[3] the transition state for quenching is probably distinct from that for bond formation (eq 4). In eq 4, exciplex formation

$$K^* + t\text{-DCE} \xrightarrow{k_c} [K\cdots t\text{-DCE}]^* \xrightarrow{k_d} K + t\text{-DCE} \quad (4)$$

$$\downarrow k_{ox}$$

oxetane

occurs with rate constant k_c and the exciplex can dissociate to give ground-state olefin and ketone with rate constant k_d or form oxetane with rate constant k_{ox}. The separation of the quenching and bond formation transition states on the reaction coordinate may make them subject to different steric or electronic influences. If this is the case, there may be no direct relationship between the rates of quenching via endo and exo attack and the efficiency of product formation resulting from these interactions.

The quantum yield for oxetane formation via eq 4 (ϕ_{ox}) will depend on the efficiency of trapping ketone singlets (ϕ_c) and the efficiency of product formation from the exciplex (ϕ_{ox}^*):

$$\phi_c = \frac{k_c[\mathrm{DCE}]}{k_c[\mathrm{DCE}] + 1/\tau_s} \quad (5)$$

$$\phi_{OX}^* = k_{ox}/(k_{ox} + k_d) \quad (6)$$

$$\phi_{ox} = \phi_c\phi_{ox}^* \quad (7)$$

For asymmetric ketones such as the 2-norbornanones, it may be possible to separate the relative rates of attack on the two faces and the efficiency of oxetane formation from each route of attack. The quantum yields from endo and exo attack are given by

$$\text{exo attack: } \phi_{ox}^x = \phi_c \frac{k_c^x}{k_c^x + k_c^n} (\phi_{ox}^*)_x \quad (8)$$

$$\text{endo attack: } \phi_{ox}^n = \phi_c \frac{k_c^n}{k_c^x + k_c^n} (\phi_{ox}^*)_n \quad (9)$$

where k_c^x and k_c^n are the rate constants for exo and endo attack, respectively ($k_c = k_c^x + k_c^n$) and $(\phi_{ox}^*)_x$ and $(\phi_{ox}^*)_n$ are the effi-

(1) Brown, H. C.; Muzzio, J. *J. Am. Chem. Soc.* **1966**, *88*, 2811.
(2) (a) Waddell, W. H.; Turro, N. J.; Farrington, G. *Mol. Photochem.* **1976**, *7*, 475. (b) See: Turro, N. J.; Farrington, G. *J. Am. Chem. Soc.*, preceding paper in this issue.
(3) (a) Turro, N. J.; Wriede, P. A.; Dalton, J. C. *J. Am. Chem. Soc.* **1968**, *90*, 3274. (b) Dalton, J. C.; Wriede, P. A.; Turro, N. J. *Ibid.* **1970**, *92*, 1318.
(4) (a) Turro, N. J.; Wriede, P. A. *J. Org. Chem.* **1969**, *34*, 3562. (b) Barltrop, J. A.; Carless, H. A. J. *J. Am. Chem. Soc.* **1972**, *94*, 1951.

0002-7863/80/1502-6056$01.00/0 © 1980 American Chemical Society

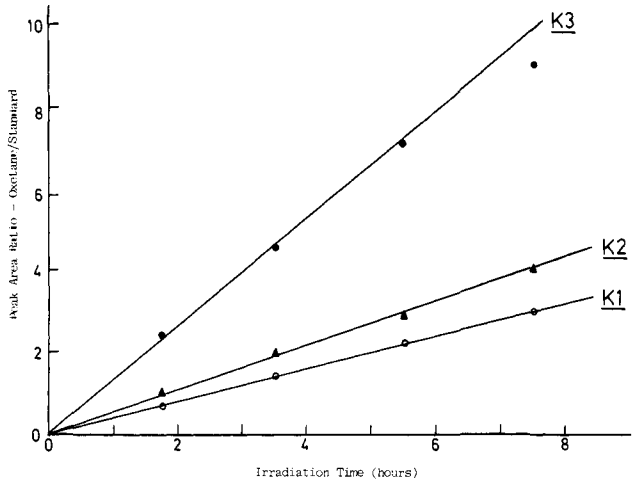

Figure 1. Plot of oxetane formation vs. time for the irradiation of **K1**, **K2**, and **K3** plus *t*-DCE through a 313-nm filter solution.

Table I. Relative Quantum Yields for Oxetane Formation between **K1**, **K2**, and **K3** and *t*-DCE

ketone	k_q^f(*t*-DCE), $M^{-1}s^{-1}$ [a]	τ_s, ns[a]	ϕ_c [b]	ϕ_{ox} [c]	ϕ_{ox}^* [c,d]
K1	5.1×10^9	5.7	0.97	1.0	1.0
K2	4.7×10^9	5.9	0.96	1.3	1.3
K3	1.0×10^9	5.0	0.83	2.9	3.4

[a] k_q^f and τ_s values from ref 2a. [b] $\phi_c = k_q^f[t\text{-DCE}]/(k_q^f[t\text{-DCE}] + 1/\tau_s)$; values of ϕ_c calculated for [*t*-DCE] = 1 M. [c] Relative to norcamphor. [d] $\phi_{ox}^* = \phi_{ox}/\phi_c$.

ciencies of oxetane formation from the endo and exo exciplexes. Then the product ratio is

exo oxetane/endo oxetane =

$$\phi_{ox}^x/\phi_{ox}^n = (k_c^x/k_c^n)((\phi_{ox}^*)_x/(\phi_{ox}^*)_n) \quad (10)$$

The overall efficiency of oxetane production arising from exo or endo attack will, therefore, depend on the efficiency with which each exciplex goes on to an oxetane as well as the rate constant for exciplex formation. Unlike the $NaBH_4$ reductions, the approach leading to favored product formation may not be the less hindered one even though complex formation is governed by steric approach control.

The lack of a predictable relationship between fluorescence quenching rates and product structure makes the determination of the stereochemistry of the oxetanes formed with *t*-DCE important. This may lead to information concerning the effects of steric hindrance on the later stages of the cycloaddition.

Relative Quantum Yields

Quantitative measurements of the relative efficiencies for oxetane formation between **K1**–**K3** and *t*-DCE were made by simultaneously irradiating equally absorbing solutions of ketone and olefin through a 313-nm filter solution on a merry-go-round apparatus. The ketone concentrations were adjusted to give each solution an optical density of 2.5. All solutions were 1 M in *t*-DCE. Aliquots were removed from the photolysis mixtures at hourly intervals and analyzed by GLC by comparison with an internal standard, generating the conversion vs. time curves shown in Figure 1. The amount of oxetane produced was found to increase linearly with time up to an irradiation period of about 7 h, at which point a yellow color began to develop in each solution, accompanied by a gradual decrease in the rate of product formation.

The relative quantum yields for oxetane formation (ϕ_{ox}) are presented in Table I, along with the ketone singlet lifetimes (τ_s) and the rates of fluorescence quenching by *t*-DCE (k_q^f). The efficiency ϕ_c with which the ketone singlets are quenched may be calculated from eq 5 by substituting k_q^f for k_c:

$$\phi_c = \frac{k_q^f[\text{DCE}]}{k_q^f[\text{DCE}] + 1/\tau_s} \quad (11)$$

Table II. Photoproduct Oxetane Designations

Ketone	Glpc Peak	Product Oxetanes
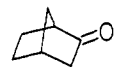 **K1**	P1*	OX(1)
	P1*	OX(7)
	P2	OX(2)
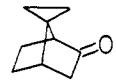 **K2**	P3*	OX(3)
	P3*	OX(8)
	P4	OX(4)
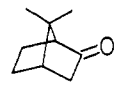 **K3**	P5*	OX(5)
	P5*	OX(9)
	P6	OX(6)

* In each case, the first product peak eluting from the glpc was found (NMR) to be a mixture of two oxetanes.

The efficiency ϕ_{ox}^* with which an exciplex partitions between cycloaddition and deactivation is thus

$$\phi_{ox}^* = k_{ox}/(k_{ox} + k_d) = \phi_{ox}/\phi_c \quad (12)$$

The quantity ϕ_{ox}^* refers to the limiting quantum yield for the cycloaddition.

The data in Table I show that, *although an increase in steric hindrance toward exo approach to the carbonyl reduces the rate of fluorescence quenching by t-DCE, the efficiency of oxetane formation from the exciplex is increased.* The k_q^f for **K3** is a factor of 5 lower than for **K1**, but ϕ_{ox}^* is more than a factor of 3 higher. It thus appears that, when a quenching interaction does occur for the more hindered ketones, the exciplex is more likely to partition toward product formation than in the less hindered cases.

Determination of Photoproduct Oxetane Structures

GLC analysis and NMR spectra provide evidence for the formation of at least three product oxetanes from the irradiation of each of the bicyclic ketones **K1**–**K3** with *t*-DCE and uncollected minor VPC peaks which may represent a fourth oxetane. The products collected and characterized are designated **OX(1)**, **OX(2)**, etc., and are identified with their corresponding GLC peaks in Table II.

Four possible trans oxetanes may be produced for the cycloaddition of *t*-DCE to a given bicyclic ketone—two from exo attack on the carbonyl (a and a′ in Figure 2) and two from endo attack (b and b′). An equal number of oxetanes having a cis stereochemistry for the nitrile groups are also possible. It can be seen from Figure 2 that eq 8 and 9 were actually presented in a simplified form, since, even if only the formation of trans oxetanes is considered, a complete description of the reaction kinetics would include terms for each of the possible olefin orientations. The efficiency of product formation from each orientation depends on both the rate constant for complex formation and the ϕ_{ox}^* for that orientation.

Assignment of structures to the photoproducts from **K1**–**K3** and *t*-DCE is based on the determination of (1) the cis/trans stereochemistry of the nitrile groups on the oxetane ring; (2) the endo/exo stereochemistry of the oxetane oxygen; (3) the configuration of the nitrile groups in relation to the norbornyl ring system—e.g., a vs. a′ for trans oxetanes with an endo oxygen.

The question of cis or trans oxetane nitrile group stereochemistry, which has implications regarding the reaction stereospecificity, will be considered first, followed by the data relating to points (2) and (3), which bear on the route of attack leading to favored product formation.

Table III. Intersystem Crossing Efficiencies for K1–K3 under Preparative Photolysis Conditions

ketone	$1/\tau_s$, s^{-1}	k_q^f[t-DCE], s^{-1} [a]	ϕ_{ST} [b]
K1	1.75×10^8	12.75×10^9	0.01
K2	1.70×10^8	11.75×10^9	0.01
K3	2.0×10^8	2.5×10^9	0.07

[a] Values for [t-DCE] = 2.5 M. [b] $\phi_{ST} = (1/\tau_s)/(k_q^f[t\text{-DCE}] + 1/\tau_s)$.

Evidence for Trans-Oxetane Formation

Under the reaction conditions for the photocycloadditions of **K1–K3** to *t*-DCE, it is unlikely that efficient cis–trans isomerization of the olefin could occur. The efficiency of generating triplets depends on the relative rates of bimolecular quenching of the singlet by *t*-DCE (rate = k_q^f[*t*-DCE]) and unimolecular decay via intersystem crossing (rate = k_{ST}). The initial concentration of *t*-DCE in preparative photocycloadditions was 3.0–4.0 M. It was calculated that in most experiments the concentration of *t*-DCE would not fall below 2.5 M even if 100% conversion to oxetanes took place. Assuming a minimum value for the bimolecular quenching rate of k_q^f (2 M) this may be compared with $1/\tau_s$ as an upper limit for k_{ST}, since $1/\tau_s = k_{ST} + k_d^f + k_f + k_r^1$. Such comparisons are summarized in Table III for **K1–K3**. At 2.5 M *t*-DCE about 99% of the norcamphor singlets, 99% of the 7,7-dimethylenenorcamphor singlets, and 93% of the 7,7-dimethylnorcamphor singlets will be trapped, and the intersystem crossing efficiencies ϕ_{ST} thus range from 0.01 to 0.07.

In addition to inefficient generation, the availability of ketone triplets to sensitize olefin isomerization is reduced by other efficient pathways for decay. The α-cleavage reaction for norcamphor triplet proceeds with $k_\alpha = 1.7 \times 10^{10}$ s^{-1},[5] while the rate of triplet quenching by *t*-DCE is $k_q^f = 5 \times 10^9$ M^{-1} s^{-1}. Even at 4.0 M *t*-DCE, only about half of the ketone triplets generated would be trapped. Thus the low ϕ_{ST} under the reaction conditions and the efficient α-cleavage from the 2-norbornanone triplets make it likely that isomerization of the *t*-DCE to *c*-DCE will be relatively unimportant. Experimentally, a slow buildup of *c*-DCE can be observed, but the cis olefin remains a very minor constituent of the photolysis mixture even at long irradiation times.

The amount of oxetanes formed from *t*-DCE and *c*-DCE would be expected to parallel their relative concentrations if the rates of quenching and product formation efficiencies are comparable for the two olefins. The fluorescence of norcamphor is quenched by *t*-DCE with a rate constant $k_q^f = 5.1 \times 10^9$ M^{-1} s^{-1} and by *c*-DCE with $k_q^f = 4.4 \times 10^9$ M^{-1} s^{-1}. The limiting quantum yields for cycloaddition of acetone to *t*-DCE and *c*-DCE were 0.076 and 0.086, respectively.[3] The comparable reactivity and oxetane formation efficiency for *t*-DCE and *c*-DCE in these cases imply that the amount of product derived from *c*-DCE should not be disproportionate to its relative concentration in the reaction mixtures.

The oxetanes from **K1–K3** under the experimental conditions used are expected from the foregoing discussion to arise from stereospecific cycloaddition to *t*-DCE to give trans products. The magnitudes of the coupling constants for the oxetane ring protons in the cycloadducts confirm the expected trans stereochemistry.[4,5] In accord with the Karplus equation,[6] the cyanooxetanes **OX(1)–OX(7)** in Table IV have coupling constants between protons with trans stereochemistry of 6.3–6.7 Hz, whereas protons in a cis configuration have coupling constants of 8.3–9.0 Hz. The coupling constants for **OX(1)–OX(9)**, as shown in Table V, fall within the range 5.1–6.8 Hz, consistent with a trans stereochemistry.[7] The broader range of *J* values in the present oxetane series may result from steric interactions which distort the oxetane ring and lead to larger variations in the dihedral angle between coupled protons.

(5) Dalton, J. C.; Dawes, K.; Turro, N. J.; Weiss, D. S.; Barltrop, J. A.; Coyle, J. D. *J. Am. Chem. Soc.* **1971**, *93*, 7213.
(6) Karplus, M. *J. Am. Chem. Soc.* **1963**, *85*, 2870.

Table IV. Proton Chemical Shifts and Coupling Constants for Cyanooxetanes

	Oxetane		Ha (δ)	Hb (δ)	J_{cis} (Hz)	J_{trans} (Hz)	Ref.
1	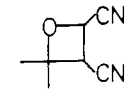	t	5.18	3.96	---	6.5	4a
		c	5.28	4.02	8.5	---	4a
2	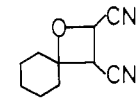	t	5.13	3.69	---	6.3	4a
		c	5.25	3.79	8.8	---	4a
3	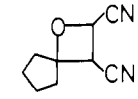	t	5.20	4.12	---	6.5	4a
		c	5.28	4.27	8.5	---	4a
4	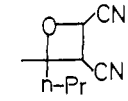	t	5.18,5.13[a]	3.88,3.83[a]	---	6.5	4a
		c	5.29,5.22[a]	4.00,3.96[a]	9.0	---	4b
5	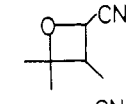	t			---	6.5	4b
		c			8.5	---	4b
6	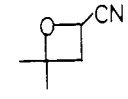				8.3	6.3	4b
7	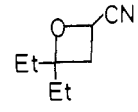				8.9	6.7	4b

[a] Positional isomers at the α' carbon (methyl, n-propyl) not assigned.

Table V. Oxetane Ring Proton Coupling Constants for Photoproducts

ketone	oxetane	J_{H_8,H_9}, Hz
K1	OX(1)	5.8
	OX(2)	6.7
	OX(7)	6.1
K2	OX(3)	6.2
	OX(4)	6.0
	OX(8)	6.3
K3	OX(5)	5.1
	OX(6)	5.6
	OX(9)	6.8

The conclusion that all of the observed product oxetanes have trans stereochemistry is thus supported by (1) the known stereospecificity of the cycloaddition in other cases; (2) the predominance of *t*-DCE under the reaction conditions; (3) the invariance of product ratios with irradiation time; (4) the coupling-constant values for the products.

Oxetane Configurations

The retention of trans stereochemistry in the photocycloaddition of **K1–K3** with *t*-DCE is consistent with the formation of four trans product oxetanes. The structural assignment of the products collected was investigated via spectroscopic methods, including ^1H NMR and ^{13}C NMR.

Oxetanes **OX(10)**, **OX(11)**, and **OX(12)** were synthesized to

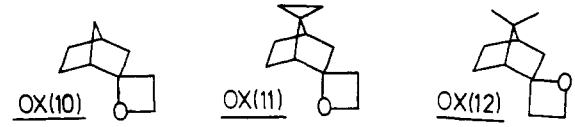

serve as model systems for the NMR studies. For these oxetanes, the oxygen configuration is predictable from the stereochemistry of ground-state nucleophilic additions and was confirmed through NMR studies.

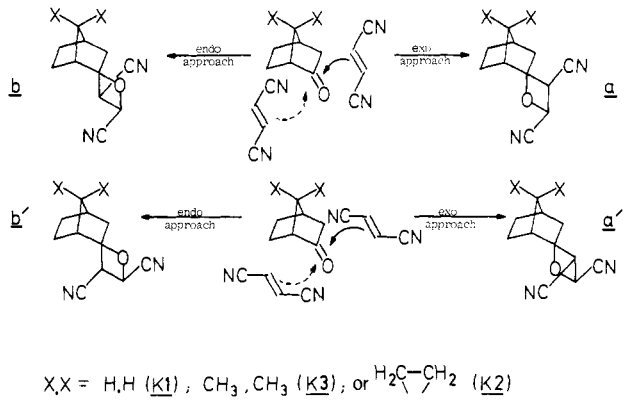

X,X = H,H (K1); CH_3,CH_3 (K3); or H_2C-CH_2 (K2)

Figure 2. Possible structures for photoproduct oxetanes.

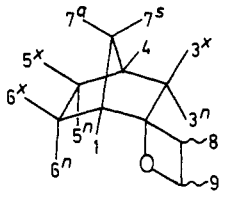

OX(1), OX(2), OX(7), OX(10)

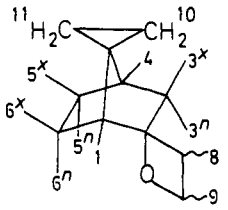

OX(3), OX(4), OX(8), OX(11)

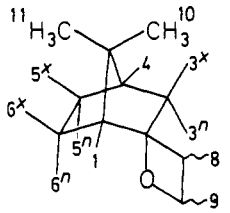

OX(5), OX(6), OX(9), OX(12)

Superscripts: n = endo
x = exo
s = syn
a = anti

Figure 3. Oxetane positional numbering.

For the major product oxetanes from **K1**–**K3** and *t*-DCE, **OX(1)**–**OX(6)**, the resonances of the oxetane ring protons (H_8 and H_9), Figure 3, and the protons at the 1,3-exo, and 3-endo positions (H_1, H_3^x, and H_3^n) could be clearly distinguished, appearing at chemical shifts generally well separated from other peaks in the spectra.[7] In addition, the cyclopropyl protons in the oxetanes derived from **K2** and methyl-group protons in products from **K3** could be identified. Only the oxetane ring protons and the cyclopropyl or methyl resonances were assignable for the minor oxetane products **OX(7)**–**OX(9)**; other resonances were obscured by those of **OX(1)**–**OX(3)**, the major components of the same VPC peak.

The identification of H_1, H_3^x, and H_3^n peaks is facilitated by their characteristic splitting patterns, which arise as a result of geminal, vicinal, and long-range couplings with other protons on the norbornane framework. The coupling constants for these interactions have been extensively investigated. A comparison of the chemical-shift data for photoproduct oxetanes derived from **K1**–**K3** and the corresponding unsubstituted oxetanes reveals the following:

(1) The introduction of cyano-group substituents at C_8 and C_9 results in a downfield shift in the positions of H_8 and H_9 by about 1.3–1.6 and 0.65–0.85 ppm, respectively, as expected from the electron-withdrawing nature of the nitrile group. In addition, the nitrile groups affect the chemical shifts of protons attached to more remote carbons on the bicyclic framework, e.g., H_1, H_3^x, and H_3^n, are generally shifted to lower τ values by amounts which vary among the isomers. These shifts presumably result from the anisotropic effect exerted by the cyano groups, which have shielding and deshielding regions similar to those of the acetylene triple bond.

(2) For the major product oxetanes derived from ketones with syn 7 substituents (**K2** and **K3**), the isomer where H_3^x is deshielded is found in greater proportion. This isomer is expected to have structure a, which brings the nitrile and H_3^x into closest proximity. Models indicate that exo approach of *t*-DCE in the orientation leading to a is more hindered than that for a′. If exo attack of *t*-DCE occurs for **K2** and **K3** to give a and a′ as the major product structures, the favored formation of a would be consistent with the observation that increased exo steric hindrance appears to increase the efficiency of oxetane formation.

(3) The chemical shifts of H_8 for the minor isomers **OX(7)**–**OX(9)** are very similar (δ 4.06–4.8) and appear 0.13–0.16 ppm downfield from H_8 of the major oxetane products. These data are consistent with an environment for H_8 in the minor isomers different from that in the major isomers, which might correspond to an endo configuration for C_8 and an exo oxygen in the oxetanes **OX(7)**–**OX(9)**.

^{13}C NMR Spectra

Natural abundance ^{13}C NMR spectra of the photoproduct oxetanes and unsubstituted oxetanes **OX(10)**–**OX(12)** were obtained at 25.2 MHz, using the pulsed method in combination with Fourier transform analysis. Noise and single-frequency off-resonance decoupling were used to simplify spectra and aid peak identification. Assignment of resonances in the ^{13}C NMR spectra of **OX(1)**–**OX(6)** was straightforward, based on the unsubstituted oxetanes **OX(10)**–**OX(12)** and the cyanooxetane **OX(13)** as model systems. The chemical-shift data are summarized in Table VI. The positions of two sets of resonances are particularly useful in the structure determination of **OX(1)**–**OX(6)**: C_6 and C_8 with regard to the oxetane endo/exo stereochemistry and C_1 and C_3 with regard to the nitrile group configuration.

The chemical shifts of the C_6 and C_8 carbons in **OX(1)**–**OX(6)** all fall within relatively narrow ranges; C_8 appears at δ 41.0–42.8, which compares closely to the β carbon in **OX(13)**, and the C_6 resonance appears between δ 18.5 and 20.1. The difference between the chemical shifts of C_6 and C_8 for isomeric pairs of oxetanes (e.g., **OX(1)** and **OX(2)**) is less than 0.5 ppm for C_6 and 0.7 ppm for C_8.

The close agreement between the chemical shifts for C_6 and C_8 argues strongly that the oxetane oxygen stereochemistry in **OX(1)**–**OX(6)** is the same. The resonance of the endo C_8 methylene group in **OX(12)** is shifted upfield by 4.8 ppm from the position of the exo C_8 in **OX(10)** as a result of steric interaction with the endo C–H at C_6. An even larger shielding might be expected for an endo C_8 in structures b and b′ in comparison with the exo C_8 of a and a′ since C_8 is part of the bulkier –CHCN

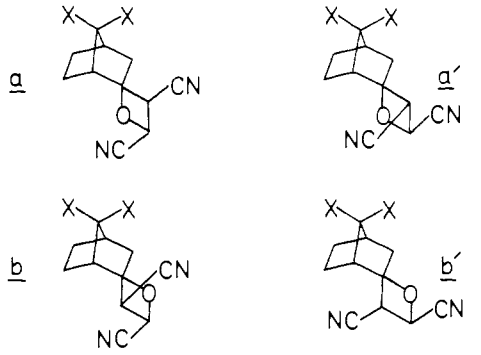

grouping and would be subject to increased steric interference in the endo configuration. In addition, a larger shielding of C_6 would be predicted for isomers with structure b′ owing to interaction with the cyano group. The absence of significantly increased

(7) Pople, J. A.; Schneider, W. G.; Bernstein, J. H. In "High Resolution Nuclear Magnetic Resonance"; McGraw-Hill, New York, 1959; Chapter 6.

Table VI. ^{13}C Chemical Shifts of Photoproducts and Model Oxetane Systems

		Chemical Shift (δ)									
		C_1	C_2	C_3	C_4	C_5	C_6	C_7	C_8	C_9	C_{10},C_{11}
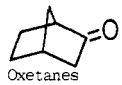 Oxetanes	OX(10)	47.4	92.4	46.8	36.9	28.7	19.9	35.9	36.9	64.3	---
	OX(1)	48.8	93.3	41.9	35.9	28.2	19.7	36.9	41.0	62.1	---
	OX(2)	44.2	92.7	46.8	36.3	28.0	19.3	36.6	41.2	61.8	---
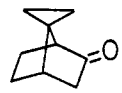 Oxetanes	OX(11)	52.1	92.6	47.6	42.7	28.6	20.4	32.9	37.3	64.5	4.1,5.0
	OX(3)	48.8	93.1	47.9	43.0	27.5	19.9	33.3	41.5	62.0	4.6,5.2
	OX(4)	53.3	93.3	42.4	42.2	28.4	20.1	32.6	41.5	62.5	4.2,4.8
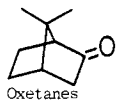 Oxetanes	OX(12)	54.2	94.6	48.8	45.2	27.4	20.7	47.4	32.0	64.2	22.0,22.1
	OX(5)	55.6	94.7	42.7	44.7	27.5	19.0	47.7	42.1	62.9	21.5,21.7
	OX(6)	51.9	96.1	47.3	45.6	27.0	18.5	47.8	42.8	62.5	21.3,22.5
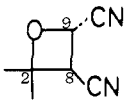 OX(13)			86.2						39.4	62.8	

shieldings of C_6 or C_8 for any of the isomers thus supports the conclusion that the major product oxetanes all have an endo oxygen stereochemistry.

The pattern of sterically induced shieldings for C_1 and C_3 which result from interactions with the nitrile groups is also consistent with structures a and a′ for the major photoproduct oxetanes. In one member of each isomeric pair C_1 is more shielded as a result of steric crowding and in the other isomer C_3 is more shielded as summarized: **OX(1)** vs. **OX(2)**, C_3 shielded 4.9 ppm in **OX(1)**, C_1 shielded 4.6 ppm in **OX(2)**; **OX(3)** vs. **OX(4)**, C_3 shielded 5.5 ppm in **OX(4)**, C_1 shielded 4.5 ppm in **OX(3)**; **OX(5)** vs. **OX(6)**, C_3 shielded 4.6 ppm in **OX(5)**, C_1 shielded 3.7 ppm in **OX(6)**. These data are in agreement with the structural assignments tentatively made for **OX(1)**–**OX(6)** from the ^1H NMR results. When a cyano group is near C_3 as in structure a, H_3^x is deshielded in the ^1H NMR and C_3 shielded in the ^{13}C NMR. Likewise, when a cyano group is near C_1 as in structure a′, H_1 is deshielded in the ^1H NMR and C_1 shielded in the ^{13}C NMR.

It was not possible to assign minor oxetane product resonances in the ^{13}C NMR. However, the conclusion that the major photocycloaddition products arise from exo attack of *t*-DCE on the carbonyl to give endo oxetanes suggests that the minor components **OX(7)**–**OX(9)** are exo oxetanes with structures corresponding to b or b′, and that the uncollected longer retention time VPC peak may represent the other exo oxetane.

Discussion

The available evidence from the ^1H and ^{13}C NMR experiments is consistent with a stereospecific cycloaddition of *t*-DCE to **K1**, **K2**, and **K3**, resulting in the formation of two major oxetane products in each case, via an exo attack on the carbonyl. From more limited data, it is concluded that the two minor products formed in each reaction are trans oxetanes from the endo attack of *t*-DCE on the carbonyl.

Although increasing steric hindrance toward exo approach of *t*-DCE to the carbonyl decreases the rate of fluorescence quenching, the proportion of products arising from endo attack apparently is not increased, in contrast to the $NaBH_4$ reduction results. The spectral data are consistent with an endo oxetane stereochemistry for the major photoproducts from **K3** as well as those from **K1** and **K2**. The lack of a significant directive effect of the syn 7-methyl in **K3** might be explained in part by the puckering of the n,π* state leading to enhanced exciplex formation from the exo face compared to the planar ground state carbonyl.

In addition, the increasing steric hindrance to exo approach actually appears to enhance the efficiency of oxetane formation with *t*-DCE (Table I); for example, the relative quantum yield for **K3** is a factor of 3.4 higher than that for **K1**. This behavior

Table VII. Fluorescence Quenching and Oxetane Formation between Acetone and α,β-Unsaturated Nitriles

	Nitrile	k_c($M^{-1}sec^{-1}$)	ϕ^*_{ox}
8		1.5×10^8	0.20
9	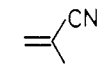	1.5×10^8	0.091
10		1.5×10^7	0.050
11		$<10^7$	~0

is opposite to that found in other cycloadditions which presumably follow a similar mechanistic pathway (eq 4), but for which the rate of exciplex formation (k_c) is found to parallel the cycloaddition efficiency (ϕ^*_{ox}). In the cycloaddition of acrylonitrile (**8**), methacrylonitrile (**9**), and crotononitrile (**10**) to acetone, interactions between β substituents on the nitrile and the acetone methyl groups are thought to be particularly important in reducing the rate of complex formation and the efficiency of oxetane formation (Table VII); β,β-dimethylacrylonitrile (**11**) does not measurably form oxetane with acetone.

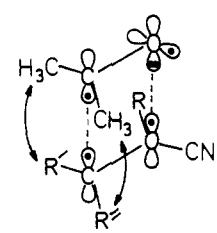

Since a similar orientation for the olefin and ketone π system is necessary to obtain in exciplex formation and bond formation, it is reasonable that k_c and k_{ox} should be subject to similar steric influences. Steric interactions which tend to reduce k_c should also increase the activation energy for bond formation and result in a decrease of k_{ox} relative to k_d, resulting in a reduction in $\phi^*_{ox} = k_{ox}/(k_{ox} + k_d)$.

Table VIII. Quantum Yields for Oxetane Formation between 2-Norbornanones and *t*-DCE

No.	Ketone	ϕ_{ox}	ϕ^*_{ox}(a)	ϕ^*_{ox}(rel.)(b)	$\Delta H^{\ddagger}_{ox}-\Delta H^{\ddagger}_{d}$(f) (kcal/mole)	Ref.
K1	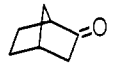	0.062	0.083	1.0	1.4	c,d
K5	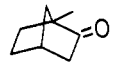	0.024	0.041	0.49	1.9	c,d
K4	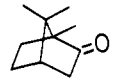	0.025	0.070	0.84	1.6	c,d
K2	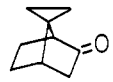	----	0.11	1.3	1.3	e
K3	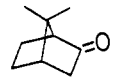	----	0.28	3.4	0.6	e

(a) $\phi^*_{ox} = k_{ox}/(k_{ox} + k_d)$
(b) Relative to Norcamphor = 1.0.
(c) J.C. Dalton, Columbia University, unpublished data.
(d) Quantum yields measured using benzophenone/benzhydrol actinometry; initial concentrations: 0.1 M t-DCE, 0.5 M ketone.
(e) ϕ^*_{ox} calculated using relative values from Table I.
(f) $\Delta H^{\ddagger}_{ox} - \Delta H^{\ddagger}_{d} = 1.38 \log_{10}(1/\phi^*_{ox} - 1)$ see text.

Preliminary quantum yield measurements on oxetane formation between *t*-DCE and norcamphor (**K1**), 1-methylnorcamphor (**K5**), and camphor (**K4**) appeared to correlate with fluorescence quenching rates in a similar manner.[8] However, the reported ϕ_{ox} were determined at 0.1 M *t*-DCE concentrations, and partly reflected differences in the efficiency of trapping the ketone singlets. The limiting quantum yields ϕ^*_{ox} were therefore recalculated. The recalculated ϕ_{ox} and the ϕ^*_{ox} are presented in Table VIII for **K1**–**K5**. The ϕ^*_{ox} values for **K1** and **K3** are calculated from the relative values and the ϕ^*_{ox} measured for norcamphor. The results indicate that a 1-methyl group reduces the efficiency of oxetane formation from the exciplex, but that the introduction of 7,7-dimethyl substitution increases ϕ^*_{ox} by a factor of 1.7 in **K4** vs. **K5** and a factor of 3.4 in **K3** vs. **K1**.

Steric effects on product distributions are found to parallel those on the overall cycloaddition efficiency. The major products **OX(4)** and **OX(5)** are formed via the more hindered of the possible configurations for exo approach by *t*-DCE, i.e., a rather than a′.

Experimental Section

Apparatus. Proton nuclear magnetic resonance spectra were taken on Varian A-60A (60 MHz), HA-100 (100 MHz), and HR-220 (220 MHz) spectrometers. The data reported were recorded at 60 MHz unless otherwise specified. ^{13}C NMR spectra were taken using the pulsed Fourier-transform method on a JEOL JNM-PS-100 high-resolution NMR spectrometer (25.2 MHz), and scans were accumulated with a Nicolet 1080 data system. For both nuclei, chemical shifts are reported in parts per million downfield from an internal tetramethylsilane standard (Me_4Si δ 0.0); coupling constants are reported in hertz.

Infrared spectra were recorded on a Perkin-Elmer Model PE-137 grating spectrophotometer. Ultraviolet absorption spectra were recorded using Cary 17 or Cary 360 spectrophotometers, and fluorescence spectra were taken at an angle of 90° from the excitation beam on a Perkin-Elmer MPF-2A fluorescence spectrophotometer. Solutions for UV and fluorescence determinations were contained in calibrated (1.00 cm^2) cells of optical grade quartz.

Preparative GLC separations were carried out using a Varian Aerograph 90P gas chromatograph with thermal conductivity detector. Quantitative analyses were performed on a Varian Series 1200 or Hewlett-Packard F & M 5750 research chromatograph with a flame ionization detector. In some cases the supports were rendered more inert toward the compounds to be separated via base washing and/or treatment with dimethyldichlorosilane (DMCS).

Elemental analyses were performed by Galbraith Laboratories, Inc., Knoxville, Tenn.

Irradiations on a preparative scale were carried out in an internally water-cooled quartz reactor at 15–25 °C with a Hanovia Type L-679A-36 450-W medium-pressure mercury arc lamp. Filter sleeves were used to absorb the shorter wavelengths during irradiations. Irradiated solutions were contained in quartz tubes fastened to the side of the reactor or in a quartz annulus which fit around the cyclindrical portion of the reactor well.

Materials. General. All commercially obtained chemicals were reagent or spectrophotometric grade and were not purified further prior to use unless otherwise specified.

Norcamphor (K1) and camphor (K4) were purchased from commercial sources.

1-Methylnorcamphor (K5) was prepared from norcamphor by the method of Bartlett and Singer.[9]

Synthesis of Spiro[cyclopropane-1,7′-norbornan]-2′-one (K2) and 7,7-Dimethylnorcamphor (K3). Spiro[cyclopropane-1,7′-norborn-5′-en]-2′-one (12). A mixture of 26.6 g of spiro[cyclopropane-1,1′-cyclopenta-2,4-diene][10] and 26.4 g of 1-chloroacrylonitrile was stirred at 100 °C for 5 h. Distillation afforded 42.2 g (81%) of 2′-chloro-2′-cyanospiro[cyclopropane-1,7′-norborn-5′-ene] (**13**), bp 75–80 °C (0.5 mm), as a clear oil which crystallized on standing: NMR (Me_4Si internal standard, CCl_4) δ 0.3–1.1 (m, 4 H, cyclopropyl), 1.78 (d, 1 H, J = 13.0 Hz, H^n_3), 2.42 (bs, 1 H, H_4), 2.85 (bs, 1 H, H_1), 2.86 (2 d, 1 H, J = 13.0 and 4.0 Hz, H^x_3), 6.18 (m, 1 H, olefinic), 6.48 (m, 1 H, olefinic); IR (CCl_4) ν_{max} 3110, 3010, 2230, 1435, 1415 cm^{-1}.

To a mixture of 17.3 g of KOH in 70 mL of ethylene glycol was added 10.1 g of **13** and the mixture stirred at 95 °C for 20 h.[11] The reaction mixture was then poured into 250 mL of water containing 10% NaCl and extracted with 6 × 100 mL of pentane. The extracts were combined, washed with water, and dried over $MgSO_4$. The solvent was removed at atmospheric pressure, leaving a yellow oil which was distilled, bp 90–92 °C (21 mm), to give 4.7 g (63%) of **12** as a clear oil (lit. bp 85 °C (13 mm):[10] NMR (Me_4Si internal standard, CCl_4) δ 0.60 and 0.63 (2 s, 4 H, cyclopropyl), 2.0 (m, 2 H, H^x_3 and H^n_3), 2.42 (m, 2 H, H_1 and H_4), 6.13 (m, 1 H, olefinic), 6.52 (m, 1 H, olefinic); IR (film) ν_{max} 3020, 1740, 745, 710 cm^{-1}.

Spiro[cyclopropane-1,7′-norbornan]-2′-one (K2). To a solution of 3.9 g of **12** in 50 mL of 95% ethanol was added 150 mg of 10% Pd/C and the mixture hydrogenated in a Parr shaker (50 psi H_2 pressure) for 6 h. The catalyst was filtered off and the ethanol removed at atmospheric pressure to give 3.25 g of **K2** as an oil which solidified on standing: mp 62–64 °C (lit.[10] 64 °C); NMR (Me_4Si internal standard, CCl_4) δ 0.55 (m, 4 H, cyclopropyl), 1.5–2.5 (m, 8 H); IR (CCl_4) ν_{max} 3020, 1745 cm^{-1}; UV (CH_3CN) λ_{max} 295 nm (ϵ 59).

7,7-Dimethylnorcamphor (K3). To a solution of 1.75 g of **K2** in 50 mL of acetic acid was added 400 mg of PtO_2 and the mixture hydrogenated in a Parr shaker (50 psi H_2 pressure) for 18 h. Following filtration to remove the catalyst, the acetic acid solution was neutralized by the addition of solid $NaHCO_3$. The neutral solution was then diluted with water and extracted with petane. The pentane extracts were washed with water, dried over $MgSO_4$, and concentrated at atmospheric pressure to give a semisolid, which was sublimed (75 °C at 10 mm) to afford 1.4 g of **K3** as a solid: mp 108–110 °C (lit.[12] 109–111 °C); NMR (Me_4Si internal standard, CCl_4) δ 1.03 (s, 6 H, methyls), 1.2–2.3 (m, 8 H); IR (CCl_4) ν_{max} 1740, 1410, 1385, 1365, 1175, 1070 cm^{-1}; UV (CH_3CN) λ_{max} 292 nm (ϵ 29).

Purification of Materials. Relative Quantum Yield Determinations. Acetonitrile. Matheson Coleman and Bell (MCB) 99+ Chromatoquality or Fisher reagent grade acetonitrile was purified by the method of O'Donnell et al.[13] To approximately 2.5 L of acetonitrile in a 5 L round-bottom flask were added 30 g of Na_2CO_3 and 45 g of $KMnO_4$. The mixture was heated and stirred for 2 h, then rapidly distilled. The first 300 mL was discarded and the remaining 2.2 L collected in a dried flask. Sufficient concentrated H_2SO_4 was added to reduce the pH below 3.0, and a white precipitate formed. The acidified acetonitrile was allowed to stand for 1 h, and the precipitate was then filtered off and the acetonitrile distilled through a 3-ft column packed with glass helices at

(8) Turro, N. J.; Dalton, J. C.; Farrington, G.; Niemczyk, M.; Pond, D D. *J. Am. Chem. Soc.* **1970**, 92, 6978.

(9) Bartlett, P. D.; Singer, G. D. *J. Am. Chem. Soc.* **1965**, *87*, 1297.
(10) Alder, K.; Ache, H. J.; Flock, F. H. *Chem. Ber.* **1960**, *93*, 1888.
(11) (a) Nelson, G. Ph.D. Thesis, University of Wisconsin (Madison), 1968. (b) Ipaktschi, J. *Tetrahedron Lett.* **1969**, 2153.
(12) (a) Lightner, D. A.; Beavers, W. A. *J. Am. Chem. Soc.* **1971**, *93*, 2677. (b) Abraham, N. A. *Ann. Chim. (Paris)* **1960**, *5*, 961.
(13) O'Donnell, J.; Ayers, J.; Mann, C. *Anal. Chem.* **1965**, *37*, 1161.

a rate of 10–15 mL/h. A forerun of about 300 mL was discarded, and the remaining 1.5–2.0 L collected in dried containers. The MCB material purified as above was UV transparent down to 230 nm. Even better results could be obtained starting with the Fisher acetonitrile; the only observable absorptions were small peaks at about 210 and 190 nm.

***trans*-1,2-Dicyanoethylene (*t*-DCE).** Commercial material (Aldrich) contained an impurity with λ_{max} (CH_3CN) ~270 nm and a significant tail absorption extending above 313 nm which could not be removed by sublimation. The *t*-DCE was therefore dissolved in a minimum amount of acetone and chromatographed on a column of Wolem neutral alumina by eluting with 3:1 pentane/ether. The middle fractions (about 75–80% of the initial amount) were combined and sublimed to give *t*-DCE with no observable absorption above 250 nm.

Bicyclic ketones **K1–K12** were purified by preparative GLC (12 ft × $^1/_4$ in. 20% XF-1150 on Chromosorb P; CT = 100–120 °C) and microdistilled or sublimed prior to use.

Procedure for Relative Quantum Yield Determinations. A merry-go-round apparatus was used to ensure the simultaneous irradiation of several samples with the same light intensity over a period of time. The apparatus consisted of an electrically driven turntable which revolved around a light source. Holes in the turntable rim were designed to accommodate test tubes containing the samples to be irradiated. The entire turntable was placed in a large water bath which maintained a constant temperature (25 ± 2 °C) during the irradiation. The light source, a Hanovia Type L-679A-36 450-W medium-pressure mercury arc lamp, was contained in a water-cooled quartz reactor fitted with a Pyrex filter sleeve. The reactor was surrounded by a Pyrex immersion well jacket containing a 313-nm filter solution (0.002 M K_2CrO_4 in a 1% aqueous solution of K_2CO_3).

The samples to be irradiated were placed in 10 × 75 mm Pyrex test tubes (Corning) which had been cleaned with Chromerge solution, washed with aqueous NH_4OH, thoroughly rinsed with distilled water, and oven dried. The test tubes were stoppered with serum caps.

Solutions of norcamphor, 7,7-dimethylnorcamphor, and spiro[cyclopropane-1,7′-norbornan]-2′-one in purified acetonitrile were prepared and the optical density was adjusted to 2.5. Aliquots of 1 mL were placed into test tubes containing 78.4 mg of *t*-DCE to provide a concentration of 1 M in the olefin. Following irradiation for 6 h through the 313-nm filter solution, an internal standard, *p*-nitroanisole (PNA), was added to each test tube and the solutions were analyzed by GLC (6 ft × $^1/_8$ in. 2% Carbowax 20M on Chromosorb G, CT = 120°C). The amount of each oxetane formed was calculated from previously determined response factors for the Varian Series 1200 flame ionization detector. Since all solutions absorbed equal amounts of light, the relative molar amounts of the oxetanes formed were taken as a measure of ϕ_{ox}.

Photolysis of Acetone and *t*-DCE. Preparative. A relatively high concentration of *t*-DCE (4 M) was employed to favor the formation of the trans oxetane. Thus, a solution of 7.8 g of *t*-DCE in 25 mL of spectrograde acetone was placed in a quartz annulus and irradiated for 96 h through a Corex filter. The solvent was removed from the dark red solution on the rotary evaporator and the residue distilled under vacuum; fractions collected at bp 98–103 °C (3 mm) were combined, allowed to solidify, and recrystallized from ether/hexane to give 6.5 g of pure trans oxetane with spectral values identical with those reported.[14]

Photolysis of Norcamphor (K1), Spiro[cyclopropane-1,7′-norbornan]-2′-one (K2), and 7,7-Dimethylnorcamphor (K3) with *t*-DCE. Preparative. The procedure employed for the photolysis of norcamphor with *t*-DCE is typical of that used for the other ketones. Thus, 1.1 g of norcamphor and 3.1 g (4 M) of *t*-DCE were dissolved in a mixture of 2 mL of methanol and 8 mL of acetonitrile (both spectrograde) which was acidified with 2–3 drops of concentrated H_2SO_4. The solution was placed in a quartz tube with ground-glass stopper and irradiated for 65 h through a Corex filter sleeve. The resulting dark red solution was shaken with saturated Na_2CO_3 solution to neutralize the acid and the solvent removed by rotary evaporation. The residue was chromatographed on a silica gel column by eluting with 4:1 petroleum ether/ether, and the presence of oxetanes in the eluted fractions monitored by GLC (10 ft × $^1/_4$ in. 2% Carbowax 20M on Chromosorb G, CT = 205 °C). The fractions containing oxetanes were combined and concentrated and the residue was fractionally sublimed under vacuum. The *t*-DCE and norcamphor sublimed at lower temperatures, and a mixture of oxetanes was collected as a solid subliming at 90–100 °C (2 mm). Preparative irradiations were carried out as above on **K1–K3** for periods of 48–96 h, and overall yields of a mixture of oxetane isomers following workup were 40–55%.

Purification of the oxetane products was carried out via preparative GLC (oxetanes from **K1** and **K3** with a 10 ft × $^1/_4$ in. 10% Carbowax 20M on DMCS-treated Chromosorb G column, CT = 205 °C; oxetanes from **K2** with a 10 ft × $^1/_4$ in. 10% XF-1150 on DMCS-treated Chromosorb G column, CT = 200 °C).

Synthesis of Oxetanes OX(10), OX(11) and OX(12). Ethyl *exo*-(2-Hydroxynorbornan-2-yl)acetate (14). Ethyl lithioacetate was prepared and reacted with norcamphor by a modification of the procedure of Rathke.[15] A solution of 14.9 g of bis(timethylsilyl)amine (a slight excess over 0.091 mol) in 90 mL of dry tetrahydrofuran was placed in a 500-mL three-necked flask equipped with nitrogen inlet tube, stopcock, and rubber septum, and stirred under a nitrogen atmosphere while 39.6 mL of a 2.3 M solution of butyllithium in hexane was added slowly by syringe. A water bath was used to cool the mixture during the addition, and the stopcock was opened periodically to permit the escape of the butane gas produced by the reaction. When the addition was complete, the flask was warmed for 15 min at 50 °C to drive off any residual butane. The resulting solution of lithium bis(trimethylsilyl)amide was cooled to −78 °C in a dry ice/acetone bath and 8.75 mL (0.091 mol) of ethyl acetate added in 0.5-mL aliquots by syringe over a 10-min period. The mixture was then stirred for 15 min at −78 °C to complete the formation of the ethyl lithioacetate.

A solution of 10 g of norcamphor (0.091 mol) in 10 mL of tetrahydrofuran was added to the stirred solution of ethyl lithioacetate at −78 °C over a 15-min period, and the mixture stirred for another 15 min. The mixture was then hydrolyzed with 20 mL of 1:1 concentrated HCl in water and warmed to room temperature. The organic layer which resulted was taken up in pentane, separated, washed with saturated NaCl solution, and dried over $MgSO_4$. Removal of the solvent at atmospheric pressure and distillation of the residue afforded 15.5 g (87%) of **14** as a colorless liquid, bp 83 °C (0.8 mm), whose spectral properties were in agreement with those previously reported:[16] NMR (Me_4Si internal standard, CCl_4) δ 1.28 (t, J = 7.0 Hz, $-COOCH_2CH_3$), 2.46 (s, 2 H, $-CH_2CO_2Et$), 3.40 (s, 1 H, OH), 4.13 (q, 2 H, J = 7.0 Hz, $-COOCH_2CH_3$); IR ν_{max} (CCl_4) 3390, 1720, 1185 cm^{-1}.

***exo*-2-(2-Hydroxyethyl)norbornan-2-ol (15).** A mixture of 2.75 g of $LiAlH_4$ (slightly more than a twofold excess) and 100 mL of dry ether was heated with refluxing of the ether for 1 h to dissolve most of the hydride, and 14 g of **14** was added dropwise with stirring at a rate sufficient to maintain a gentle reflux of the solvent. The mixture was refluxed for an additional 6 h, then cooled to room temperature. The sequential addition of 2.75 mL of water, 2.75 mL of 15% aqueous NaOH, and finally 8.25 mL of water resulted in a copious, white precipitate, which was separated by filtration and washed several times with ether. The ether solution was dried over $MgSO_4$ and the solvent removed. Distillation of the residue afforded 9.5 g (85%) of **15** as a clear, viscous oil, bp 120–122 °C (1 mm), which solidified on standing to a waxy solid: mp 26–28 °C; NMR (Me_4Si internal standard, $CDCl_3$) δ 1.78 (t, J = 5.5 Hz, $-C(OH)CH_2-$), 3.08 (bs, 2 H, OH), 3.90 (t, 2 H, J = 5.5 Hz, $-CH_2OH$); IR ν_{max} (CCl_4) 3425 (sh), 3250, 1070 cm^{-1}.

Spiro[norbornane-2,2′-oxetane] (OX(10)). The monobrosylate of diol **15** was prepared by dissolving 1.17 g of **15** (0.00755 mol) and 1.98 g of *p*-bromobenzenesulfonyl chloride in separate 7-mL portions of dry pyridine, cooling both solutions to below −5 °C in an ice–salt bath, and quickly mixing them.[17] The mixture was placed in the freezer (−21 °C) and allowed to react for 19 h. The cooled mixture was covered with a layer of ether and stirred and the layers were separated. The aqueous layer was extracted with three portions of ether, which were combined with the separated ether layer, washed with saturated $NaHCO_3$ solution, and dried over $MgSO_4$. Removal of the ether by rotory evaporation afforded 2.8 g of a cloudy, light orange oil, the monobrosylate ester of the primary hydroxyl, which was used without further purification.

The crude oil was dissolved in 20 mL of a 1 N solution of potassium *tert*-butoxide in *tert*-butyl alcohol and stirred at room temperature for 20 h. The copious, white precipitate which formed was dissolved with the addition of water and a dilute HCl solution was added until the mixture reached pH 8. The mixture was then extracted with three portions of benzene, and the organic layers were combined, washed with saturated aqueous NaCl solution, and dried over calcium hydroxide. The benzene was removed at atmospheric pressure in the presence of $Ca(OH)_2$, and the residue distilled using base-washed glassware to give 725 mg of colorless liquid, bp 75–77 °C (6 mm). Analysis by GLC (6 ft × $^1/_4$ in. 20% Apiezon L on base-washed Chromosorb P, CT = 145 °C) indicated that the distillate contained approximately 90% pure oxetane **OX(10)**, and a pure sample was isolated by preparative GLC under the same conditions: NMR (Me_4Si internal standard, CCl_4) δ 1.1–1.9 (m, 8 H, norbornane system), 2.16 (bs, 1 H, H_4), 2.40 (bs, 1 H, H_1), 2.48

(14) Beereboom, J. J.; vonWittenau, M. S. *J. Org. Chem.* **1965**, *30*, 1231.

(15) Rathke, M. W. *J. Am. Chem. Soc.* **1970**, *92*, 3222.

(16) Luria, F.; Vecchietti, V.; Logemann, W.; Tosolini, G.; Dradi, E. *Tetrahedron* **1969**, *25*, 3989.

(17) Henbest, H. B.; Millward, B. B. *J. Chem. Soc.* **1960**, 3575.

(t, 2 H, J = 7.5 Hz, $-OCH_2CH_2-$), 4.39 (t, 2 H, J = 7.5 Hz, $-OCH_2CH-$); IR ν_{max} (CS_2) 980, 965 cm^{-1}. Anal. Calcd for $C_9H_{14}O$: C, 78.12; H, 10.21. Found: C, 77.99; H, 10.10.

Ethyl *exo*-(2′-Hydroxyspiro[cyclopropane-1,7′-norbornan]-2′-yl)acetate (16). To a solution of 0.0367 mol of ethyl lithioacetate in tetrahydrofuran at −78 °C was added a solution of 5.0 g of spiro[cyclopropane-1,7′-norbornan]-2′-one (**K2**) in 5 mL of tetrahydrofuran over a 15-min period, and the mixture was stirred for 30 min in the cold. Following hydrolysis of the lithium salt and workup as described above, the product was distilled, bp 94–96 °C (0.8 mm), to give 6.5 g (80%) of a colorless liquid. Analysis by GLC (6 ft × 1/4 in. 20% Apiezon L on base-washed Chromosorb P, CT = 165 °C) indicated a purity of ~98% **16**: NMR (Me_4Si internal standard, CCl_4) δ 0.5 (m, 4 H, cyclopropyl), 1.25 (t, J = 7.0 Hz, $-COOCH_2CH_3$), 2.63 (s, 2 H, $(CH_3)_2C(OH)CH_2COOEt$), 3.45 (s, 1 H, OH), 4.15 (q, 2 H, J = 7.0 Hz, $-COOCH_2CH_3$); IR ν_{max} (CCl_4) 3390, 2990, 1710, 1185 cm^{-1}.

***exo*-2′-(2-Hydroxyethyl)spiro[cyclopropane-1,7′-norbornan]-2′-ol (17).** Reduction of 6.0 g of ester **16** with $LiAlH_4$ in ether under the conditions described above afforded on workup 4.25 g (88%) of **17** as a thick oil: bp 120–122 °C (0.7 mm); NMR (Me_4Si internal standard, $CDCl_3$) δ 0.5 (m, 4 H, cyclopropyl), 1.95 (t, J = 5.5 Hz, $(CH_3)_2C(OH)CH_2-$), 3.0 (position concentration dependent, bs, 2 H, OH), 3.90 (t, 2 H, J = 5.5 Hz, $-CH_2OH$); IR ν_{max} (CCl_4) 3450 (sh), 3250, 3010, 1065 cm^{-1}.

Dispiro[cyclopropane-1,7′-norbornane-2′,2″-oxetane] (OX(11)). Formation of the monobrosylate ester of **17** from 3.8 g of the diol and 5.5 g of *p*-bromobenzenesulfonyl chloride followed by ring closure with potassium *tert*-butoxide in *tert*-butyl alcohol was carried out as described for **15**. Distillation of the resulting residue afforded 2.8 g of a clear liquid, bp 95–96 °C (0.5 mm), which was analyzed by GLC and found to consist of approximately 90% pure oxetane **OX(11)**. A pure sample was isolated by GLC (10 ft × 1/4 in. 2% Carbowax 20M on base-washed Chromosorb G): NMR (Me_4Si internal standard standard) δ 0.4 (m, 4 H, cyclopropyl), 2.09 (2 q, 1 H, major splitting J = 13.0 Hz, H_3^x), 2.57 (t, 2 H, J = 7.5 Hz, $-O-CH_2CH_2-$), 4.40 (t, 2 H, J = 7.5 Hz, $-O-CH_2-$); IR ν_{max} (CS_2) 3030, 1005, 980, 965, 955 cm^{-1}. Anal. Calcd for $C_{11}H_{16}O$: C, 80.44; H, 9.82. Found: C, 80.30; H, 9.89.

Ethyl *endo*-(7,7-Dimethyl-2-hydroxynorbornan-2-yl)acetate (18). To a solution of 0.0289 mol of ethyl lithioacetate in tetrahydrofuran at −78 °C was added a solution of 4.0 g of 7,7-dimethylnorcamphor in tetrahydrofuran over a 15-min period, and the mixture allowed to stir for 4 h in the cold. Following workup in the usual manner distillation of the residue gave, in addition to 2.2 g of starting ketone, 1.7 g of **18** as a clear liquid: bp 130–134 °C (6 mm); NMR (Me_4Si internal standard, CCl_4) δ 0.97 and 1.32 (2 s, each 3 H, 7-CH_3's), 1.25 (t, 3 H, J = 7.0 Hz; $-COOCH_2CH_3$), 2.51 (s, 2 H, $(CH_3)_2C(CH_2-)OH$), 3.43 (3, 1 H, OH), 4.15 (q, 2 H, J = 7.0 Hz, $-COOCH_2CH_3$); IR ν_{max} (CCl_4) 3355, 1725, 1380, 1360 cm^{-1}.

***endo*-2-(2-Hydroxyethyl)-7,7-dimethylnorbornan-2-ol (19).** Reduction of 2 g of ester **18** with $LiAlH_4$ in ether afforded after workup 1.5 g of **19** as a thick oil: bp 125–127 °C (0.5 mm); NMR (Me_4Si internal standard $CDCl_3$) δ 1.02 and 1.33 (2 s, each 3 H, 7-CH_3's), 1.83 (t, J = 5.5 Hz, $(CH_3)_2C(CH_2-)OH$), 3.4 (bs, 2 H, OH), 3.85 (t, 2 H, J = 5.5 Hz, $-CH_2OH$); IR ν_{max} (film) 3330 (broad), 1380, 1360 cm^{-1}.

7,7-Dimethylspiro[norbornane-2,2′-oxetane] (OX(12)). Formation of the monobrosylate ester of **19** from 1.2 g of diol and 1.75 g of *p*-bromobenzenesulfonyl chloride and subsequent ring closure with potassium *tert*-butoxide in *tert*-butyl alchohol resulted in the formation of 510 mg of a clear liquid, bp 82–85 °C (2 mm), which was purified by preparative GLC (6 ft × 1/4 in. 20% Apiezon L on base-washed Chromosorb P, CT = 165 °C): NMR (Me_4Si internal standard, CCl_4, 100 MHz) δ 0.95, 1.07 (2 s, each 3 H, 7-CH_3's), 0.9–2.3 (m, 8 H, norbornane), 2.5 (m, 2 H, oxetane $-CH_2CH_2O-$), 4.23 (m, 2 H, oxetane $-CH_2O$); IR ν_{max} (CS_2) 1380, 1365, 990, 965 cm^{-1}. Anal. Calcd for $C_{11}H_{18}O$: C, 79.46; H, 10.91. Found: C, 79.33; H, 10.88.

Acknowledgments. The authors thank the National Science Foundation and The Air Force Office of Scientific Research for their generous support of this research.

Studies on the Spiro[2.5]octadienyl Radical and the 2-Phenylethyl Rearrangement[1]

A. Effio,[2,3] D. Griller,[3] K. U. Ingold,*[3] J. C. Scaiano,[3,4] and S. J. Sheng[4]

Contribution from the Division of Chemistry, National Research Council of Canada, Ottawa, Canada K1A 0R6, and the Radiation Laboratory, University of Notre Dame, Notre Dame, Indiana 46556. *Received June 9, 1980*

Abstract: The title radical, **5**, has been generated by hydrogen atom abstraction from spiro[2.5]octa-4,6-diene (**4**). The radical could not be observed by EPR spectroscopy even at temperatures as low as 100 K. Instead, the EPR spectrum of the cyclopropyl ring-opened product was obtained, 2-phenylethyl (**6**). However, **5** was identified by using optical detection methods by means of its absorption and fluorescence at ca. 560 nm, which is a characteristic of cyclohexadienyls. The rate constant for H atom abstraction from **4** by *tert*-butoxyl was measured at 295 K, and approximate Arrhenius parameters for the **5** to **6** rearrangement have been estimated. The hydrocarbon **4** is remarkably resistant to the thermodynamically favored, radical induced rearrangement to ethyl benzene.

The rearrangement of neophyl (**1**) to 1-phenyl-2-methylprop-2-yl (**3**) (eq 1), which was the first free-radical rearrangement

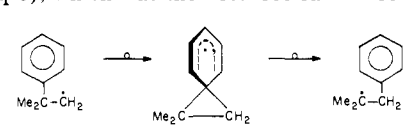

1 2 3 (1)

to be discovered,[5] continues to intrigue organic chemists.[6] Abundant evidence exists that this rearrangement is intramolecular,[6] and this implies that it must proceed via a 1,1-dimethylspiro[2.5]octadienyl radical (**2**). This might be either an intermediate or merely a transition state. Attempts to detect **2**,[7-10] and related spiro radicals,[7-9,11] by EPR spectroscopy at low tem-

(1) Issued as N.R.C.C. No. 18530; this is also publication No. NDRL-2128 from the Notre Dame Radiation Laboratory and was partially supported by the office of Basic Energy Sciences of the U.S. Department of Energy.
(2) N.R.C.C. Research Associate, 1978–1979.
(3) N.R.C.C.
(4) Radiation Laboratory.
(5) Urry, W. H.; Kharasch, M. S. *J. Am. Chem. Soc.* **1944**, *66*, 1438.
(6) For reviews of this and related rearrangements see: (a) Wilt, J. W. In "Free Radicals"; Kochi, J. K., Ed.; Wiley: New York, 1973; Vol. I, Chapter 8; (b) Beckwith, A. L. J.; Ingold, K. U. In "Rearrangements in Ground and Excited States"; de Mayo, P., Ed.; Academic Press: New York, in press.
(7) Kochi, J. K.; Krusic, P. J. *J. Am. Chem. Soc.* **1969**, *91*, 3940.
(8) Edge, D. J.; Kochi, J. K. *J. Am. Chem. Soc.* **1972**, *94*, 7695.
(9) Hamilton, E. J., Jr.; Fischer, H. *Helv. Chim. Acta* **1973**, *56*, 795.
(10) Maillard, B.; Ingold, K. U. *J. Am. Chem. Soc.* **1976**, *98*, 1224, 4692.
(11) Brunton, G.; McBay, H. C.; Ingold, K. U. *J. Am. Chem. Soc.* **1977**, *99*, 4447.

0002-7863/80/1502-6063$01.00/0 © 1980 American Chemical Society